THE ASTROPHYSICAL JOURNAL, 280:887–891, 1984 May 15

HARD X-RAY IMAGING OF THE SOLAR FLARE ON 1981 MAY 13 WITH THE *HINOTORI* SPACECRAFT

S. TSUNETA,[1] T. TAKAKURA, AND N. NITTA
Department of Astronomy, University of Tokyo

K. OHKI AND K. TANAKA
Tokyo Astronomical Observatory, University of Tokyo

K. MAKISHIMA, T. MURAKAMI, M. ODA, AND Y. OGAWARA
Institute of Space and Astronautical Science
AND

I. KONDO
Institute for Cosmic Ray Research, University of Tokyo; and Institute of Space and Astronautical Science
Received 1983 June 21; accepted 1983 August 26

ABSTRACT

Hard X-ray images and X-ray spectra of an intense solar flare that occurred at E58N09 on 1981 May 13 are presented and discussed. The observation was made with Japanese solar X-ray spacecraft *Hinotori*. An unusual hard X-ray source, observed at 14–38 keV, had a steady spatial displacement of $\sim 1'$ toward the limb from the two-ribbon Hα flare during the 16 minutes of hard X-ray observation, including the time of maximum flux. This suggests that the source was located near the top of a coronal loop structure connecting the two ribbons, at an estimated altitude of $\sim 4 \times 10^4$ km above the photosphere. The soft X-ray (5–10 keV) source nearly coincided in position and size with the hard X-ray source. Near the peak of hard X-ray time profile, $\sim 40\%$ of the total count rate of the hard X-ray image is estimated to come from a power-law component, as observed with the hard X-ray spectrometer. The parameters of the thermal plasma near the loop top were determined to be $n = 3 \times 10^{10}$ cm^{-3}, $T = 2 \times 10^7$ K, and $\beta = 16\pi nkT/B^2 \approx 1.0$. Intense heat conduction from the thermal plasma near the loop top to the transition region appears to be in equilibrium with the continuous energy release near the loop top.

Subject headings: radiation mechanisms — Sun: flares — Sun: X-rays — X-rays: spectra

I. INTRODUCTION

A two-ribbon 2B/X1.5 flare on 1981 May 13, which exhibits unique characteristics among the solar hard X-ray events, was well observed with the Japanese *Hinotori* spacecraft which was launched on 1981 February 21 by the Institute of Space and Astronautical Science (ISAS). In this paper, we describe and discuss the flare, with emphasis on the data obtained with the hard X-ray imaging telescope (SXT) on *Hinotori*. The SXT comprises a pair of rotating modulation collimators (Oda 1965; Schnopper, Thompson, and Watt 1968; Oda *et al.* 1976; Oda 1983, and references therein) with NaI scintillation detectors. A brief description of the SXT has been presented by Makishima (1982) and Takakura *et al.* (1983), with full details in Tsuneta (1983). Other *Hinotori* instruments used in the present analysis are rotating crystal spectrometers (Tanaka *et al.* 1982*a*, *b*) and a hard X-ray spectrometer (SXT/HXM team 1982). Data from Hα filtergrams obtained at the Tokyo Astronomical Observatory were also available.

Recent results on hard X-ray imaging observation showed that in some solar flares two footpoints located in regions with different magnetic polarities were bright in the impulsive phase, which suggested the presence of electron *beams* precipitating onto the transition region within both legs of a magnetic tube (Hoyng *et al.* 1981; Machado, Duijveman, and Dennis 1982; Duijveman, Hoyng, and Machado 1982; Tsuneta *et al.* 1983; Tsuneta 1983; Duijveman 1983). The present imaging observation, however, shows distinct hard X-ray characteristics compared to those quoted above. A hard X-ray flare similar to the present flare has previously been reported by Takakura *et al.* (1983).

II. OBSERVATIONS

a) Time Evolution of the Flare

The flare started at $\sim 03^h50^m$ UT and ended at $\sim 06^h10^m$ in Hα (*Solar Geophysical Data*). *Hinotori* observed the flare between 04^h01^m and 04^h28^m, including the peak of hard X-rays. Of the two hard X-ray telescopes (SXT-1 and SXT-2), SXT-1 observed the flare in a 16–38 keV band from 04^h02^m to 04^h14^m. Then its energy range was automatically switched to 5–10 keV band until 04^h18^m. SXT-2 continuously observed a 14–28 keV band until 04^h18^m. After 04^h18^m, only the total count rate of the SXT was monitored. Crystal spectrometer data were available during the same period as SXT, and hard X-ray spectra were obtained throughout the observation until 04^h28^m.

Figure 1 shows the time profiles of hard X-ray flux in four energy bands, as well as those of SXT averaged over one spin period of the spacecraft (16.7 s). The time variation of the hard X-rays was smooth and showed no impulsive component even at energies above 100 keV during the observation. The microwave time profiles at 9.4 GHz were also smooth without an impulsive component at any time during the flare (S. Enome, private communication). According to the observation at Nobeyama Solar Radio Observatory (K. Kai, private communication), type III bursts were observed between 03^h58^m and 04^h00^m, and type IV bursts between 04^h05^m and 04^h30^m with pulsations. A type II burst was not observed.

[1] Currently at Institute of Space and Astronautical Science.

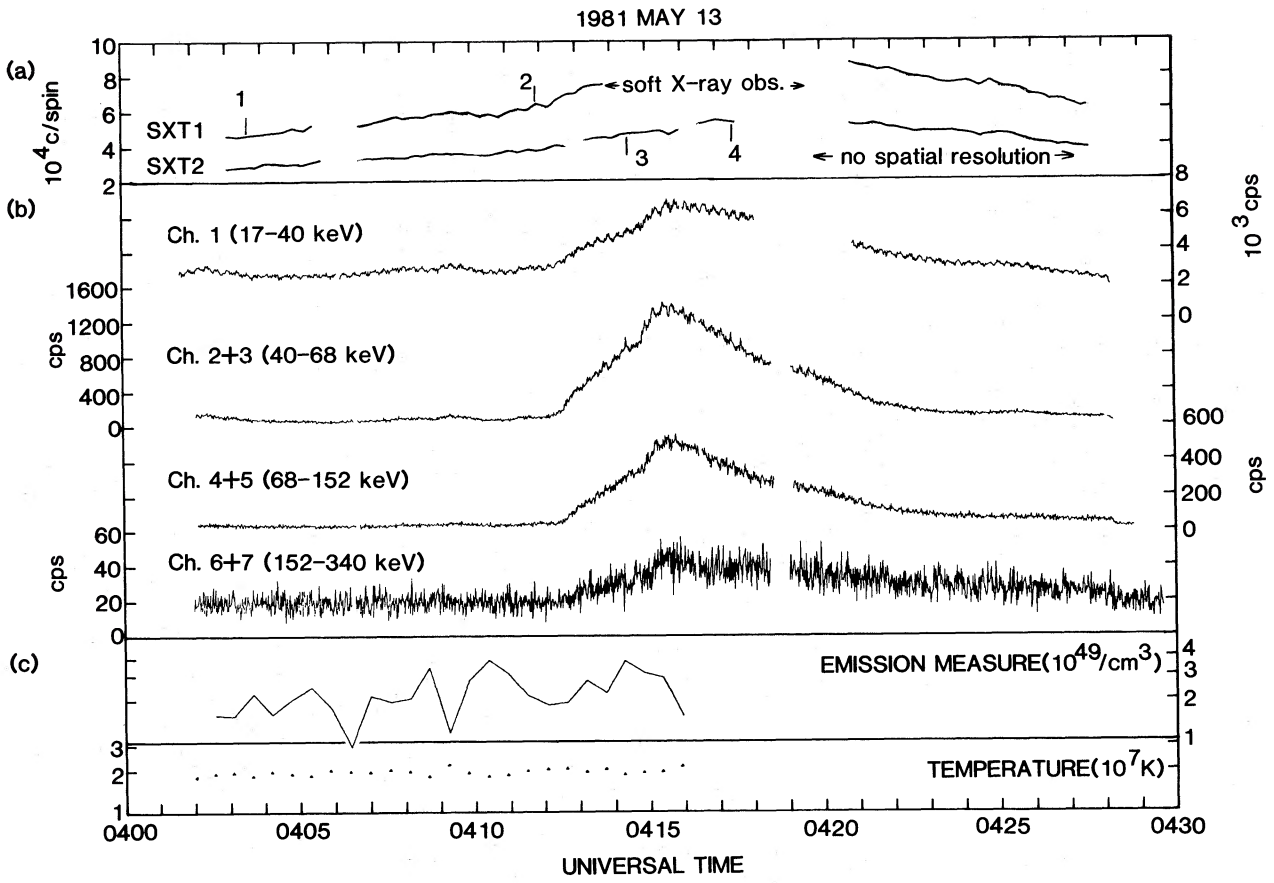

FIG. 1.—(*a*) Time profiles of the total count rates of the two hard X-ray telescopes (SXT-1 and SXT-2) after integrating over one spin period of the spacecraft (16.7 s). SXT-1 was in the 5–10 keV band from 04^h14^m UT to 04^h18^m, during which the light curve is not shown. After 04^h18^m, only the total count rates of the SXT were monitored. (*b*) Hard X-ray time profiles in four energy bands as observed by the scintillation-counter spectrometer on *Hinotori*. All data points are plotted with 1.0 s time resolution. Shallow modulation in the lower bands with period of ~17 s is due to spin rotation of the spacecraft. The count rate before 150 keV, even before 04^h12^m, is larger than the background count rate. Some part of the data in (*a*) and (*b*) are missed because of calibration and telemetry breakdown. SXT light curves follow well that of the spectrometer channel 1. (*c*) Time profiles of emission measure and temperature deduced from Fe XXV and Fe XXIV lines. Relatively large variations of the emission measure may result from the small errors in the temperature.

Spectral fitting of the spectrometer data over the range from 40 keV to 150–300 keV shows the flare photon spectrum to be fairly well represented by a single power. The spectral hardness showed a systematic tendency to increase on the average with time, most markedly on the rising phase of the hard X-ray peak from 04^h11^m to 04^h15^m. The hardening continued even in the decay phase. The photon spectral index was ~5–4.5 between 04^h02^m (start of the observation) and 04^h11^m, hardening to ~3.5 around the hard X-ray peak and to ~3 in the decay phase.

Figure 1 also shows time profiles of electron temperature and emission measure deduced from the Fe XXV and Fe XXIV lines observed with the crystal spectrometer. The temperature was constant at $\sim 2 \times 10^7$ K, and the (mean) emission measure was $\sim 2\text{–}3 \times 10^{49}$ cm^{-3}, with a slight increase on the average during the observation. Weak Fe XXVI lines can also be seen in the spectrum integrated over the entire observation (Tanaka *et al.* 1982*a*). The line ratio analysis of Fe XXVI lines indicates a relatively low temperature (2×10^7 K) of the plasma emitting Fe XXVI lines, and both Fe XXVI and Fe XXV lines appear to be emitted from the same plasma. Neither broadening nor blue-shifts of the spectral lines, which are usually seen before the hard X-ray peak, were found.

Observation with the gamma-ray spectrometer aboard *Hinotori* showed that the gamma-ray peak in energies above several hundred keV had a delay of a few minutes compared with hard X-ray peak below 100 keV (Yoshimori *et al.* 1983).

b) X-Ray Imaging

Figure 2 presents hard X-ray images in the 16–38 and 14–28 keV ranges obtained with SXT-1 and SXT-2, respectively, and soft X-ray (5–10 keV) images obtained with SXT-1 near the end of the imaging observation. Hard X-ray images obtained with SXT-1 are nearly the same as those independently obtained with SXT-2. The X-ray images are produced from one-dimensional scans in ~15 directions, obtained with a rotating modulation collimator (Oda *et al.* 1976), using the maximum entropy method (Willingale 1981; Tsuneta 1983) developed for two-dimensional image reconstruction from projected images. The images are synthesized assuming that there exist no X-ray sources outside a circle with radius of 1.'6 centered on the location shown in Figure 2. Although the beam-width (fringe) is ~30″ (FWHM), the image presented here attains a resolution of ~15″ as a result of the sharp fringe pattern (Makishima 1982). The convolutions of the derived two-dimensional images with the collimator transmission function show excellent fits to

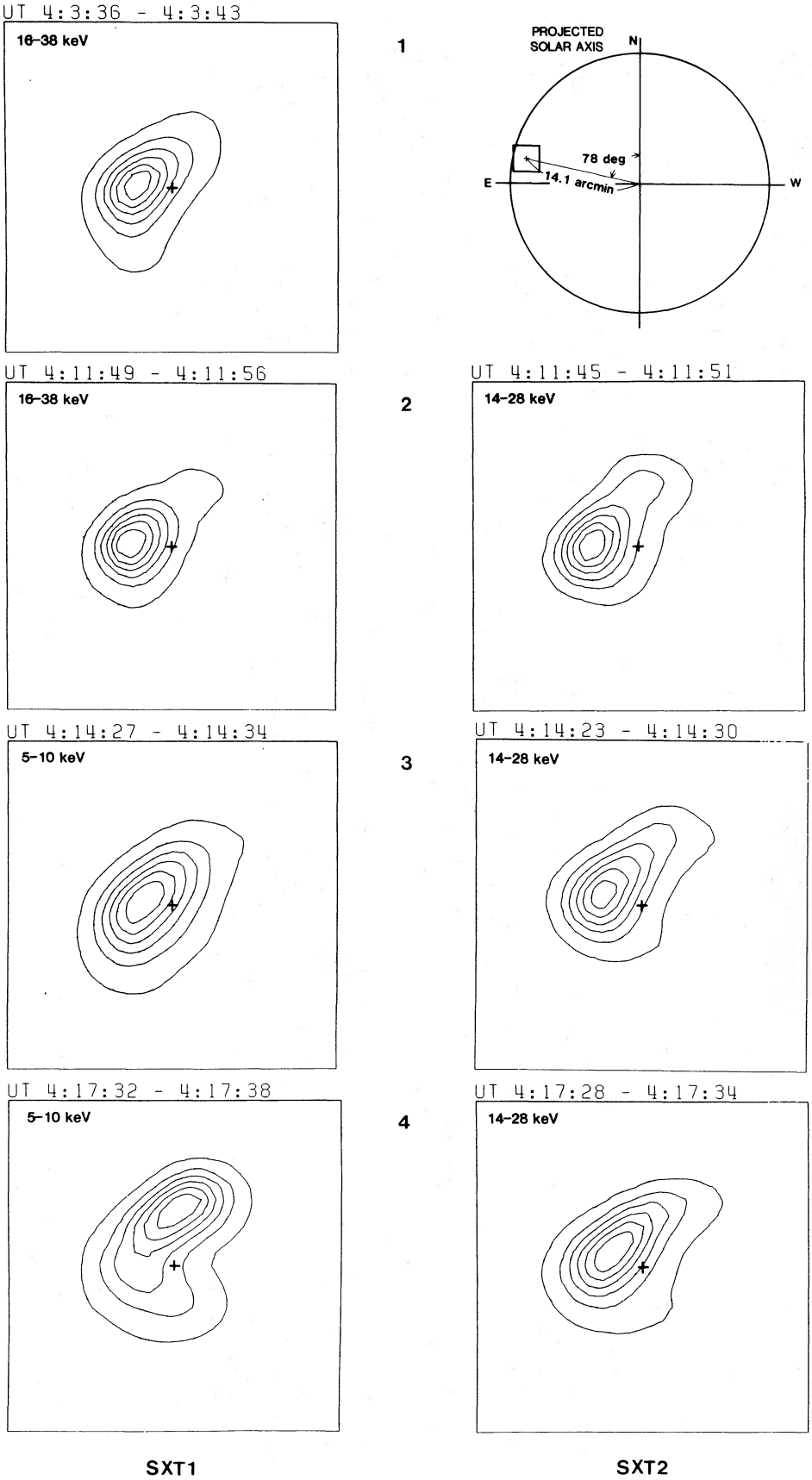

FIG. 2.—Hard X-ray images at the four times 1–4 indicated in Fig. 1, together with the soft X-ray images at times 3 and 4. The maps have a pixel size of 7.″6, and field of view is 3.′2. The intensity in each pixel is normalized to the peak intensity in each map. The contour interval is 15%, and the lowest level is 10%. The location of the map on the solar disk is indicated in the upper right.

the observed one-dimensional scans for each direction of projection.

As presented in Figure 2, the hard X-ray source was elongated in the NW-SE direction with a size $\sim 70'' \times 30''$ (FWHM). No significant time variations of the size or structure of the hard X-ray source, such as expansion or motion toward the limb, were seen during the imaging observations. The soft X-ray source nearly coincided in position and size with the hard X-ray source during the 4 minutes of soft X-ray observation including the peak of hard X-rays. The centroid of the soft X-ray emission was, however, displaced $\sim 8''$ toward the solar center[2] with respect to that of hard X-ray emission before the hard X-ray peak (panel 3 of Fig. 2). In the decay phase of hard X-rays, the centroid of the soft X-ray source moved upward and was displaced relative to that of the hard X-ray source along the limb by $\sim 30''$ (panel 4 of Fig. 2).

c) *Comparison with* Hα *Map*

Figure 3 (Plate 13) presents a hard X-ray image near the hard X-ray peak overlaid on an Hα photograph taken ~ 26 minutes after the hard X-ray observation. The global structure of the Hα flare did not change during this period. The hard X-ray source was clearly displaced from the well-developed two-ribbon flare by $\sim 1'$ toward the limb. The maximum combined positional error in the overlay is within $\sim 15''$ in radial direction on the solar disk and within $\sim 30''$ in the azimuthal direction (direction parallel to the limb). The $1'$ displacement observed is definitely larger than the upper limit of the error in the overlay. The displacement persisted throughout the observation. The hard and soft *X*-ray intensities at the location of the Hα ribbons were below 10% of the peak intensity.

After $\sim 04^h30^m$, a postflare loop-prominence system connecting the two ribbons was clearly seen (E. Hiei, private communication). Traces of this can be seen in Figure 3. The location of the top of the arcade of loops seems to coincide in position with the X-ray source of 30 minutes earlier. The displacement of the X-ray source from the Hα ribbons is considered to be due to the projection of a high-altitude coronal hard X-ray source which was stably located near the top of the coronal loop structure connecting the two ribbons during the 16 minutes of the imaging observation. Sakurai (1983) confirmed that the X-ray source was indeed located near the top of a magnetic arcade, based on the potential field calculation. If the hard X-ray source was located just above the two-ribbon flare, its height would then be $\sim 4 \times 10^4$ km above the photosphere.

III. DISCUSSION

a) *Nature of Hard X-Ray Source*

Recent microwave observations with VLA showed that in the impulsive phase of some relatively weak flares, the microwave source at high frequencies (above 10 GHz) was located in between Hα ribbons, which suggests the presence of the energetic electrons near the loop top (Marsh and Hurford 1980; Marsh *et al.* 1981). On the other hand, the hard X-ray imaging spectrometer on the *SMM* observed a coronal loop-like structure which appeared near the end of the impulsive phase following the footpoints emission, and was attributed to the hot plasma of 4×10^7 K, rather than to the nonthermal electrons (Hoyng *et al.* 1981; Duijveman 1983). Similarly, Lin *et al.* (1981) reported a hot component with a maximum temperature of 3.4×10^7 K. Furthermore, Tanaka *et al.* (1982*b*) identified a hot component emitting intense Fe XXVI lines with a peak temperature of 3.6×10^7 K. Such a hot component constitutes one class of flare plasmas located in coronal loops. It is therefore important to estimate the relative contributions of the power-law component and the thermal plasma including this hot component in the present hard X-ray image in order to understand the nature of present hard X-ray source.

The hard X-ray spectrometer aboard the *Hinotori* has a rapid decrease in efficiency below 20 keV by the use of a thick aluminum filter of 432 mg cm^{-2}, which ensures little contamination of intense soft X-rays, while SXT has an aluminum filter of 189 mg cm^{-2} in 99% of the detector area and 27 mg cm^{-2} in the remaining 1%. (Note that this allows SXT to be somewhat more sensitive to the thermal component than the spectrometer.) Accordingly, the hard X-ray spectrometer, with the aid of the soft X-ray crystal spectrometer, serves as a reference in order to estimate the thermal contamination to the SXT hard X-ray image.

The hard X-ray intensity in every channel of the spectrometer from 17 to 300 keV has similar light curves, which implies the common origin of the hard X-rays from electrons with power-law spectrum. We conclude for the following two reasons that the power-law electron spectrum extends at least down to 15 keV near the peak of hard X-ray time profile. (i) If the hard X-rays observed in the lower bands of the spectrometer were completely of thermal origin with temperature of above 3×10^7 K, this should have caused intense Fe XXVI lines detectable by the crystal spectrometer. However, only faint Fe XXVI lines were seen in the spectrum integrated over the entire observations. (ii) From the extrapolation of the power-law hard X-ray spectrum, obtained between 40 keV and 150–300 keV, down to 15 keV, we find that the count rate of the spectrometer channel 1 (17–40 keV) is almost entirely due to the power-law component near the peak of hard X-ray time profile. Then, by using this power-law spectrum folded through the proper response functions of the SXT collimator and detector, we estimate that $\sim 40\%$ of the SXT total count rate came from the power component near the peak of hard X-ray time profile, and $\sim 10\%$–20% during the plateau before 04^h12^m. This can be seen in the SXT light curves shown in Figure 1, which follow reasonably well the light curve of the spectrometer channel 1. The remainder is partly due to the thermal plasma of 2×10^7 K, and there is a possibility that higher temperatures, above 3×10^7 K, with relatively small emission measures contributes somewhat to the hard X-ray image. The present flare has, however, completely different characteristics compared to the hot thermal flares, without a significant nonthermal component such as 1981 April 2 flare (Tanaka *et al.* 1982*b*) and 1981 July 17 flare (Tsuneta 1983) observed with the *Hinotori*; these flares had enough hot thermal plasma of above 3×10^7 K with large emission measure greater than 10^{49} cm^{-3} to emit intense Fe XXVI lines, and showed a small, stationary, hard X-ray source of $\sim 10''$ (FWHM) and a relatively low altitude below 10^4 km above the photosphere.

These considerations lead us to the interpretation that a rich population of nonthermal electrons with a power-law spectrum were generated and resided within the coronal loop structure, at least near the peak of hard X-rays from 04^h11^m and

[2] Although the beam width of the SXT is $\sim 30''$ (FWHM), the relative positional accuracy between SXT-1 and SXT-2 is good to within several arc seconds (Tsuneta 1983).

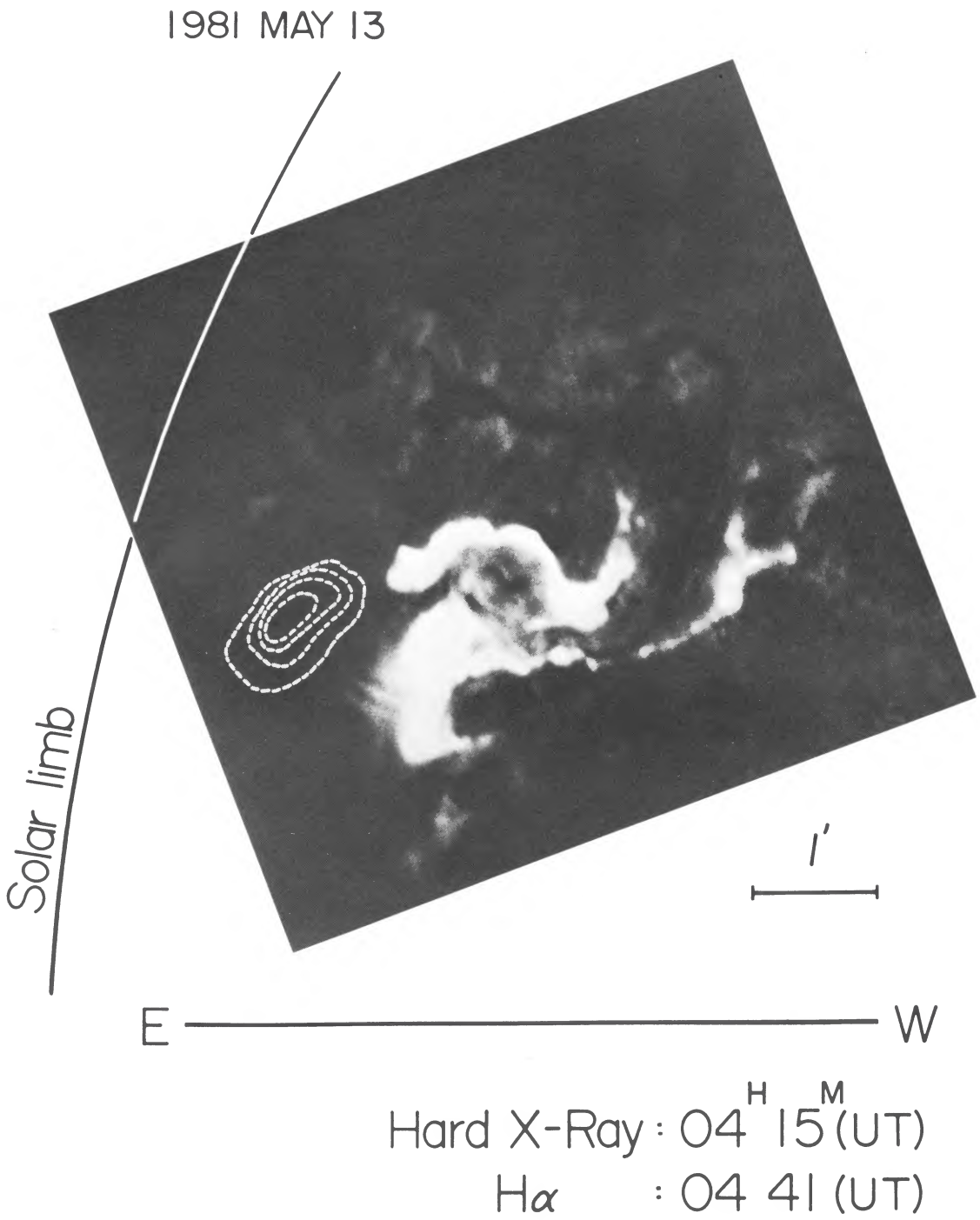

FIG. 3.—Overlay of the hard X-ray image near the peak of hard X-rays with an Hα (6562.8 Å) photograph (courtesy of E. Hiei) taken 26 minutes after the hard X-ray observation. The global structure of the Hα flare did not change during this period. The contour interval is 20%.

TSUNETA *et al.* (*see* page 890)

04^h18^m. Further evidence supporting this interpretation comes from microwave observations. One-dimensional brightness observations at 35 GHz showed that the main microwave source coincided in position with the hard X-ray source (Kawabata, Ogawa, and Suzuki 1983). The peak intensity at 35 GHz was ~ 352 sfu (1 sfu = 10^{-22} W m^{-2} Hz^{-1}), with a spectrum typical of gyrosynchrotron emission (*Solar Geophysical Data*). Free-free emission from the thermal plasma of 2×10^7 K only produced ~ 5 sfu at 35 GHz, which shows the presence of rich population of nonthermal electrons within the coronal loop.

b) *Energy Balance of the Coronal Loop*

From the soft X-ray source area S and emission measure, we find the electron density of the plasma emitting Fe XXV lines near the loop top to be 3×10^{10} cm^{-3}, assuming a volume equal to $S^{1.5}$. Since the magnetic field strength near the loop top is ~ 50 gauss, based on the potential field calculation (Sakurai 1983), the plasma $\beta = 16\pi nkT/B^2$ is nearly equal to 1.

We estimate the radiative cooling loss to be $\sim 6 \times 10^{26}$ ergs s^{-1} (Raymond, Cox, and Smith 1976) and the conductive loss to the transition region to be $\sim 1.1 \times 10^{29}$ ergs s^{-1}, assuming a tube radius of 15″ and a temperature scale length of 70″. (The saturated heat flux is $\sim 2.4 \times 10^{29}$ ergs s^{-1}.) Therefore, in order to sustain the strong heat conduction to the transition region from the loop top, continuous energy input is necessary. This energy supply is perhaps the thick-target energy loss of nonthermal electrons in the coronal loop: thick-target energy loss above 10 keV is $\sim 2 \times 10^{29}$ ergs s^{-1} near the peak of hard X-ray time profile. Actually, for electrons with energies below 30 keV, the coronal loop itself becomes a thick target without need for a specific confinement mechanism. The total energy content of the thermal plasma of 2×10^7 K is 8.3×10^{30} ergs.

c) *Relation with Metric Bursts*

This type of the flare can be classified as a gradual hard X-ray burst or extended burst because of its long duration, smooth time profile, and systematic hardening of the hard X-ray spectrum (Hoyng *et al.* 1976; Hudson 1979). In relation to second phase acceleration, the acceleration agent for the gradual hard X-ray burst was suggested to be type II shocks (Hudson, Lin, and Stewart 1982). The present flare contradicts this interpretation because of the absence of type II shocks and the steady location of the hard X-ray source. Accordingly, a shock is not the direct agent for particle acceleration in this gradual hard X-ray burst.

It was pointed out that the stationary or moving type IV burst may be a radio counterpart of extended type burst (Hudson 1978). In general, the height of the meter wave type IV burst is higher, and the size of the burst is larger (Boischot 1974) compared to the present hard X-ray source. Therefore, meter wave type IV burst would not coincide in *position* with the extended hard X-ray burst.

We thank Professor E. Hiei at the Tokyo Astronomical Observatory for kindly providing us the valuable Hα photograph.

The highly successful operation of the *Hinotori* spacecraft is the result of several years of intense work by many people. We express our special thanks to the members of the *Hinotori* project team headed by Professor Y. Tanaka of the Institute of Space and Astronautical Science (ISAS).

REFERENCES

Boischot, A. 1974, in *Coronal Disturbances*, ed. G. Newkirk, Jr. (Dordrecht: Reidel), p. 423.
Duijveman, A. 1983, Ph.D. thesis, University of Utrecht.
Duijveman, A., Hoyng, P., and Machado, M. E. 1982, *Solar Phys.*, **81**, 137.
Hoyng, P., Brown, J. C., and van Beek, H. F. 1976, *Solar Phys.*, **48**, 197.
Hoyng, P., *et al.* 1981, *Ap. J. (Letters)*, **246**, L155.
Hudson, H. S. 1978, *Ap. J.*, **224**, 235.
———. 1979, in *Proc. AIP Conf. Particle Acceleration in Astrophysics, No. 56*, ed. H. C. Wolfe (New York: Am. Institute of Physics), p. 115.
Hudson, H. S., Lin, R. P., and Stewart, R. T. 1982, *Solar Phys.*, **75**, 245.
Kawabata, K., Ogawa, H., and Suzuki, I. 1983, in *Proc. US–Japan Seminar, Recent Advances on the Understanding of Solar Flares*, ed. S. R. Kane *et al.* (*Solar Phys.*, **86**, 247).
Lin, R. P., *et al.* 1981, *Ap. J. (Letters)*, **251**, L109.
Machado, M. E., Duijveman, A., and Dennis, B. R. 1982, *Solar Phys.*, **79**, 85.
Makishima, K. 1982, in *Proc. Hinotori Symposium on Solar Flares*, ed. Y. Tanaka *et al.* (Tokyo: Institute of Space and Astronautical Science), p. 120.
Marsh, K. A., *et al.* 1981, *Ap. J.*, **251**, 797.
Marsh, K. A., and Hurford, G. J. 1980, *Ap. J. (Letters)*, **240**, L111.
Oda, M. 1965, *Appl. Optics*, **4**, 143.
———. 1983, *Adv. Space Res.*, **2**, 207.
Oda, M., *et al.* 1976, *Space Sci. Instr.*, **2**, 141.
Raymond, J. C., Cox, D. P., and Smith, B. W. 1976, *Ap. J.*, **204**, 290.
Sakurai, T. 1983, in *Proc. US–Japan Seminar, Recent Advances on the Understanding of Solar Flares*, ed. S. R. Kane *et al.* (*Solar Phys.*, **86**, 339).
Schnopper, H. W., Thompson, R. I., and Watt, S. 1968, *Space Sci. Rev.*, **8**, 534.
SXT/HXM team. 1982, *Preliminary Data from Hard X-Ray Monitor on Hinotori* (Tokyo: Tokyo Astronomical Observatory).
Takakura, T., *et al.* 1983, *Ap. J. (Letters)*, **270**, L83.
Tanaka, K., *et al.* 1982*a*, *Ann. Tokyo Astr. Obs.*, **18**, 237.
———. 1982*b*, *Ap. J. (Letters)*, **254**, L59.
Tsuneta, S. 1983, Ph.D. thesis, University of Tokyo, Japan.
Tsuneta, S., *et al.* 1983, in *Proc. US–Japan Seminar, Recent Advances on the Understanding of Solar Flares*, ed. S. R. Kane *et al.* (*Solar Phys.*, **86**, 313).
Willingale, R. 1981, *M.N.R.A.S.*, **194**, 359.
Yoshimori, M., *et al.* 1983, *Proc. 18th Internat. Cosmic Ray Conf.*, in press.

I. KONDO: Institute for Cosmic Ray Research, University of Tokyo, Tanashi, Tokyo 188, Japan

K. MAKISHIMA, T. MURAKAMI, M. ODA, Y. OGAWARA, and S. TSUNETA: Institute of Space and Astronautical Science (ISAS), Komaba, Meguro-ku, Tokyo 153, Japan

N. NITTA and T. TAKAKURA: Department of Astronomy, University of Tokyo, Bunkyo-ku, Tokyo 113, Japan

K. OHKI and K. TANAKA: Tokyo Astronomical Observatory, University of Tokyo, Mitaka, Tokyo 188, Japan